MRS Advances (2024) 9:193–198
https://doi.org/10.1557/s43580-023-00728-6

ORIGINAL PAPER

Effectiveness of green coatings as a possible protection barrier against corrosion

A. A. Aguilar-Ruiz[1] · R. G. Sánchez-Duarte[1] · G. E. Dévora-Isiordia[1] · Y. Villegas-Peralta[1] · J. Álvarez-Sánchez[1] · V. M. Orozco-Carmona[2]

Received: 14 September 2023 / Accepted: 22 November 2023 / Published online: 18 December 2023

Abstract

The increasing attention towards chitosan, a versatile polymer known for its eco-friendly nature origin, non-bio accumulative characteristics, biodegradability, and low or non-toxicity, has sparked significant interest in recent years due to its corrosion-resistant properties. This study pursues to assess the efficacy of chitosan derivatives of different molecular weights as protective green corrosion barriers. Two different molecular weight chitosan variants, high and medium molecular weight (HMW and MMW) were used, both in their pure form and crosslinked with Polyethylene Glycol (PEG), and Polyvinylpyrrolidone (PVP). The coatings were prepared using the sol–gel technique. The synthesized chitosan-based green coatings were characterized using attenuated total reflection Fourier transform infrared spectroscopy (ATR-FTIR), Atomic Force Microscope (AFM), and contact angle studies. Corrosion resistance protection was evaluated through Weight loss measurements. Contact angles obtained for all samples were 60–80° evidencing the hydrophilic behavior of the coatings. ATR-FTIR coatings spectra presented characteristic peaks of the chitosan functional groups and displayed a relevant correlation between chitosan and the agents crosslinked. The AFM results for roughness (Ra) of the samples before and after the coating process indicated a strong relation between the decrease in the roughness parameter and the enhancement of the barrier protective property. The coating's weight loss percentages do not show a significant change throughout the experiment, staying within the 0.1–0.9% range. Finally, the results reported here could serve as a reference to synthesizing green coatings for corrosion protection as an alternative to traditional corrosion inhibitors.

Introduction

Corrosion is a spontaneous and natural process of deterioration that typically affects metals. It involves a destructive attack that can occur through chemical or electrochemical reactions between the metal and its environment. This phenomenon leads to changes in properties, and, in many cases, the degradation of metallic materials found worldwide [1, 2]. Because corrosion has a substantial impact on the economy, safety, and material preservation, its investigation and mitigation are crucial [3].

Although the corrosion process cannot be completely avoided, the rate of corrosion could be efficiently reduced by using a variety of approaches, such as cathodic and anodic protection, corrosion inhibitors, barrier surface coatings, etc. One of the most used methods to prevent corrosion involves utilizing different compounds called "coatings" which are adhered over the metal surfaces and serve as physical barriers [4]. The physical barrier method provides a good corrosion protective coating that prevents electrolyte/diffusive ions from reaching the coating/metal interface [5].

The coating acts not only as an obstacle between the substrate and the corrosive environment but also as a repository for inhibitors. In general, the coatings can act as a sacrificial anode that degrades instead of the base metal [6]. The quest for materials to build coatings with a low environmental impact is therefore a constant endeavor in all spheres of human activity due to the high levels of pollution present worldwide. Therefore, researchers are actively seeking more environmentally

✉ R. G. Sánchez-Duarte
reyna.sanchez@itson.edu.mx

[1] Departamento de Ciencias del Agua y Medio Ambiente, Instituto Tecnológico de Sonora (ITSON), 5 de Febrero 818 Sur, Col. Centro, C.P. 85000 Ciudad Obregon, Sonora, Mexico

[2] Centro de Investigación en Materiales Avanzados S.C., Ave. Miguel de Cervantes 120, Complejo Industrial Chihuahua, C.P. 31136 Chihuahua, Chih., Mexico

friendly anticorrosive treatments as a current focus of research [7].

Chitosan, the deacetylated form of chitin is a naturally occurring biopolymer that is widespread in nature. The most common source of chitin extraction comes from the exoskeleton of certain species such seafood processing industry (shrimp, crabs, crustaceans, mollusks, etc.), some insects, plants, and fungi [8]. Chitosan molecular structure enables a variety of mechanical and chemical alterations that can improve or give new features to this macromolecule [9].

Chitosan is thought to have considerable potential for the development of novel materials principally because of its biocompatibility quality and its ability to maintain the original structure and size of the protected section. The development of modified chitosan-based coatings with mechanical and antibacterial qualities, which would help extend the life of metals and prevent biological fouling, is being explored as a solution to the corrosion problem [10].

Because of its qualities, including biocompatibility, antibacterial activity, non-toxicity, biodegradability, and the capacity to form effective films, there's an increasing interest in chitosan coatings studies where chitosan-based coatings can be used in a variety of industries, including the creation of biomedical materials, biosensors, the food industry, the textile business, and the cosmetics industry, among others [11].

Chitosan coatings applied to substrates using the dip coating process and other sol–gel techniques have proven to be very successful in preventing corrosion. They create thin layers with specific properties attributed to the loose, gel-like structure of the polymer in solution. Another advantage is that it allows the use of various crosslinking agents to alter the structure and enhance certain properties, such as reducing permeability and swelling, among others [12].

The present work aims to prepare and evaluate chitosan derivatives as green corrosion barriers to protect metal surfaces from aggressive environmental conditions as an alternative to traditional corrosion inhibitors. Pure chitosan (Chi), glutaraldehyde (Glu), polyethylene glycol (PEG), and polyvinylpyrrolidone (PVP) chitosan-crosslinked coatings were prepared through the sol–gel technique. The obtained coatings were characterized through attenuated total reflection Fourier transform infrared spectroscopy analysis (ATR-FTIR), atomic force microscopy (AFM), and water contact angle measurements. Corrosion resistance protection was evaluated through weight loss measurements.

Material and methods

Reagents

Stainless steel 304 plates of 5 × 5 cm purchased from a local store were utilized as test material. Chitosan was obtained from the alkaline deacetylation of chitin in shrimp shell waste following the methodology of Sánchez-Duarte et al. [13]. 99.5% Acetic acid and 99.5% Acetone were purchased from FAGA lab. Polyethylene glycol (PEG) and 37.4% Chlorohydric acid (HCl) were purchased from Merck. 25% Glutaraldehyde (Glu), and polyvinylpyrrolidone (PVP) were purchased from Sigma-Aldrich. Synthetic seawater was obtained from Instant Ocean. Reagents were used without a purification step.

The molecular weight of Chitosan was determined through intrinsic viscosity measurements and molecular structure analysis. % deacetylation, % Ash, and % humidity were carried out analysis for chitosan physicochemical characterization. Coatings were prepared according to the methodology presented by Szoke et al. [14]. Coatings were characterized by contact angle, ATR-FTIR, and AFM studies. The coating's corrosion protection inhibitory effect was assessed by gravimetric tests.

Stainless steel pretreatment

Stainless steel plates were sanded with 200, 400, 1000, 1200, and 2000 wet sandpaper to achieve a uniform surface. Subsequently, the plates underwent two rounds of ultrasonic cleaning for 10 min each in acetone solution to remove any residual metal particles from the sanding. Next, ultrasonicated plates were rinsed with distilled water and air-dried. The plates were then immersed for 30 s in 0.1 M hydrochloric acid followed by thoroughly rinse with distilled water, dried in a drying oven at 60 °C for 24 h, and stored for future use.

Coatings preparation

Two different chitosan were used, High Molecular Weight (HMW) and Medium Molecular Weight (MMW). For the pure chitosan coatings, two chitosan solutions were prepared, following the procedure outlined by Aguilar et al. [15] with slight modifications, consisting of dissolving both HMW and MMW chitosan in 2% acetic acid. From this solutions chitosan pure coatings for high and medium MW were obtained (HMW-Chi and MMW-Chi). In the case of crosslinked chitosan coatings, the solutions described above were prepared, and then PEG and Glu were added to obtain the HMW chitosan crosslinked with PEG (HMW-Chi/PEG) and the MMW chitosan crosslinked with PEG (MMW-Chi/PEG) solutions. PVP and Glu were added to the pure chitosan solutions to obtain the HMW chitosan crosslinked with PVP (HMW-Chi/PVP) and the MMW chitosan crosslinked with PVP (MMW-Chi/PVP) solutions. Subsequently, the solutions were mechanically stirred for 1 h at 400 rpm, left to rest for 24 h, and finally filtered to remove any undissolved particles.3.5% synthetic seawater was prepared by dissolving the seawater salt into distilled water.

For the preparation of the coatings, pre-treated plates were taken into the chitosan solutions and their modifications (previously described). Right after, plates were withdrawn at a rate of 5 cm/min and dried at room temperature for 24 h. All coated plates were prepared in triplicate, dried, and stored until use.

Characterization studies

Chitosan

To determine the Molecular Weight (MW) of synthesized chitosan, the intrinsic viscosity was analyzed using the method described for Masuelli using the Mark–Houwink equation (Eq. 1) where η is the intrinsic viscosity, K and an a are constants, and Mv is the average viscosimetric molecular weight. An Ubbelohde capillary viscosimeter in a thermostatic bath (300.1 °C) was used following the technique outlined by Sánchez-Duarte et al· [13], and humidity and ashes were assessed.

$$[\eta] = KM_v^a \tag{1}$$

The MW and deacetylation degree of chitosan were determined using the Fourier transform infrared spectroscopy (FTIR) recorded under dry air at room temperature within the wave number range of 400–4200 cm^{-1} with a spectral resolution of 100 cm^{-1}.

Coating samples

To ascertain the contact angle measurements, the sessile drop technique through Dataphysics equipment, model OCA 15EC, using the SCA20 1.0 software (dataphysics, Filderstadt, Germany) was evaluated. Atomic Force Microscopy (AFM workshop, Signal Hill, CA, USA) (model TT-AFM) studies were carried out to study the morphology and determine the roughness of the sample surfaces. FTIR (Thermo Scientific Spectrum model Nicolet iS5, Waltham, MA, USA) spectra were run under ATR mode to study the molecular structure of the coatings. The region ranged from 500 to 4000 cm^{-1}.

Weight loss analysis

To study the protective behavior of chitosan-based coatings, samples were exposed to an aggressive medium by placing them in flasks containing 3.5% synthetic seawater solution. The samples were withdrawn after 24 h of immersion time and then weekly for 58 days. The samples were rinsed and dried in the oven at 60 °C for 12 h followed by the weight determination and then taken back to immersion.

$$Weightloss(\%) = \frac{W_0 - W_1}{W_0} x100 \tag{2}$$

where W_0 y W_1 is the weight of the samples before and after immersion tests, respectively.

Results and discussion

Chitosan characterization

Chitosan characterization results are the following, the average MW of the chitosan was 587.11 kDa for the HMW-Chi and 397.43 kDa for the MMW-Chi, the Deacetylation (%) was > 90, the Humidity (%) ranged from 6.46 to 8.49, and Ashes (%) from 0.93 to 0.71. Reported values are the average of $n = 3$ standard deviation. The characterization results are congruent with what has been reported in the literature [11, 16, 17].

Contact angle

Contact angle values were obtained for chitosan-based coatings, results are shown in Table 1. Contact angles obtained for all samples were consistent with the reported in diverse studies (60–80°) evidencing the hydrophilic behavior of the coatings that can be attributed to the inherent hydrophilic nature of chitosan, PEG, and PVP. It is worth noting that the HMW-Chi/PEG and HMW-Chi coatings displayed higher contact angles. In contrast, MMW-Chi/PVP coatings exhibited only a slight contact angle decrease with closer values to the aforementioned. This could be attributed to a better incorporation of glutaraldehyde, a hydrophobic compound that was incorporated as a linking arm for the addition of the crosslinking agents. This incorporation prevents a significant drop in the contact angle results [12, 18]. Overall, the rest of the samples displayed a more significant decrease in contact angles. Gunbas et al. [18] associated this effect with the deformation of the chitosan structure provoked by cross-linking in film forms. This deformation leads to

Table 1 High and medium molecular weight chitosan-based coatings contact angle

Sample	Contact angle (°)
HMW-Chi	73.80 ± 3.870
HMW-Chi/PEG	73.30 ± 2.078
HMW-Chi/PVP	65.13 ± 2.023
MMW-Chi	67.90 ± 1.762
MMW-Chi/PEG	65.58 ± 3.362
MMW-Chi/PVP	70.25 ± 2.605

Reported values are the average of $n = 5$ standard deviation

changes in the conformations of the macromolecules, allowing functional groups to migrate to the surface and increase hydrophilicity.

ATR-FTIR spectra

ATR-FTIR coatings spectra are presented in Fig. 1. Characteristic peaks of the chitosan functional groups are presented [5]. Expected signals from 3200 to 3500 cm^{-1} of the O–H and N–H groups are barely detectable for HMW-Chi and MMW-Chi coatings, the previously mentioned could be explained due to an overlap of the coating with the stainless-steel plates on which coatings are deposited causing interference and noise in readings Ojeda and Dittrich. [19]. Nonetheless, it can be noted that the spectra for the HMW-Chi group and the MMW-Chi coatings present C=O, N–H, C–N, and C–O chitosan characteristic peaks corresponding to the stretching vibration bond of amide I at 1570 cm^{-1} (C=O), amino flexion vibration at 1314 cm^{-1} (N–H), amide III stretching vibration at 1318 cm^{-1} (C–N). Chitosan characteristic peaks are still present in the Chi/PEG coatings. However, some peaks appear less pronounced, indicating a modification in the chitosan structure which may be directly related to the grafting of PEG in the matrix. C=N appearing peak at 1613 cm^{-1} indicates stretching vibrations in Schiff's base from glutaraldehyde and chitosan reaction. 1283 cm^{-1} peak is attributed to the bending vibration of the O–H groups whereas 1099 cm^{-1} signal represents symmetrical and asymmetrical C–O–C stretching. Finally, the 712 cm^{-1} signal corresponds to the C–H bond, thus displaying relevant correlation between chitosan and PEG [18]. Chitosan crosslinked with PVP spectra presents the characteristic peaks of chitosan groups (C–O–C, C=O, and N–H) along with the presence of the Schift base imine group formed between the chitosan and the glutaraldehyde (C=N). 1645 cm^{-1} stretching vibration signal of the C=O exhibits PVP absorption. 1300 and 1018 cm^{-1} bands could be ascribed to the C–O and C–N (pyridine ring) stretching vibration of the PVP structure. Zhang et al. [20] and Padash et al. [21] mentioned similar spectra signals peak for PVP.

AFM

The surface morphology of the samples was evaluated. Results are shown in Table 2. A notable decrease in Average Roughness (Ra) can be observed after the coating process except for the PEG and PVP cross-linkages which may be attributed to the not well-deposited coating onto the metal surface. Coatings produce a smoother surface overall by filling in minute microscopic surface flaws when applied evenly, therefore, a decrease in the roughness parameter after the coating application may be strongly associated with a good covering of the surface by the coating enhancing surface smoothness. Similar findings were made by Alves et al. [22]. They compared different pre-treated samples before and after the coating process in terms of surface roughness and adherence, evidencing better adherence results for the coated samples that displayed roughness parameters decreased rather than increased. In other similar works, Latthe et al. [23] ascribed the decrease of the roughness parameter after coating deposition to the gaps and voids present on the plates filled and covered by the coating resulting in the decrease in the surface roughness. Thus, suggesting a potential relationship between the decreased roughness and the deposition of the coating into the valleys and peaks of the substrate's surface. A smoother surface is less likely to have pits, cracks, or places where corrosive substances can

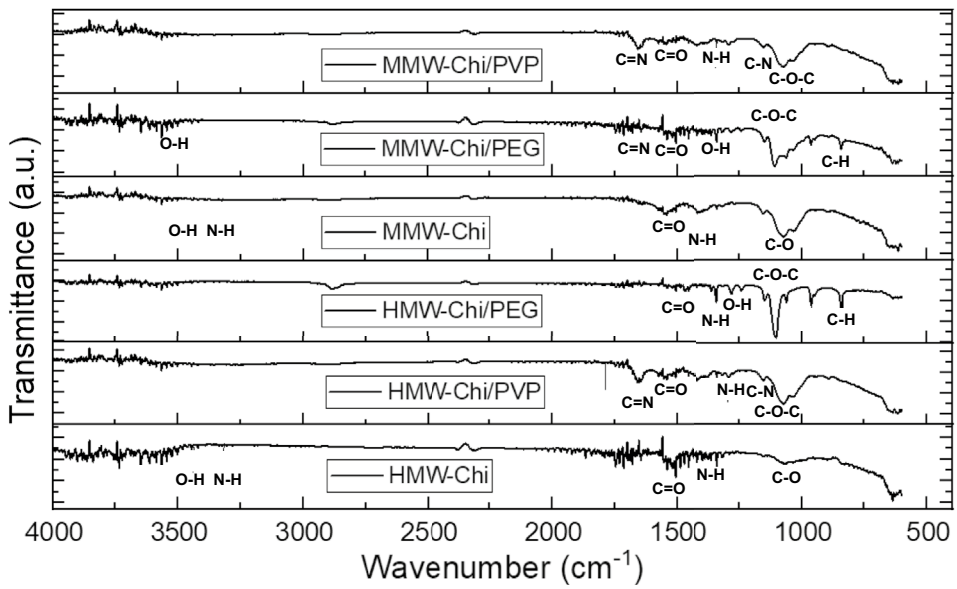

Fig. 1 ATR-FTIR medium and high molecular weight chitosan-based coatings spectra

Table 2 Surface roughness parameters of naked and medium and high molecular weight chitosan coatings on stainless steel

Sample	Ra (nm)
Stainless steel	89.90 ± 14.52
HMW-chi	21.58 ± 7.77
HMW-chi/PEG	85.22 ± 43.85
HMW-chi/PVP	72.23 ± 16.57
MMW-chi	55.71 ± 13.88
MMW-chi/PEG	78.50 ± 13.23
MMW-chi/PVP	28.63 ± 12.19

Ra is the Roughness average surface

Reported values are the average of $n = 6$ standard deviation

collect. This may have long-term effects, including a more effective corrosion defense [24, 25].

Weight loss measurements

Samples were studied by the weight loss method. The weight of the samples before and after immersion in 3.5% NaCl solution was compiled. Equation 2 earlier described in the methodology was used to determine the weight loss percentages. An average of 2 measurements was taken and the standard deviation was calculated, results are shown in Fig. 2. From the data analysis, it can be inferred that the coating's weight loss percentages do not show a significant change throughout the experiment, staying within the 0.1–0.9% range. This behavior could indicate that the coating layer was well adhered to the metal surface remaining almost intact throughout the experiment. Analogous results are presented by Motlatle et al. [4] who reported that this may be indicative of high barrier protection efficiency conferred by the coatings. MMW-Chi/PVP coatings displayed the lowest percentage of weight loss standing out among the rest of the samples. These results are consistent with the roughness data previously discussed and reinforce the hypothesis that attributes the decrease in Ra to the good adhesion of the coating onto the stainless-steel surface thus enhancing barrier protection. However, these results give an overview of the protective behavior properties of Chitosan-based coating against corrosion, signifying that more accurate methods are required to support the corrosion inhibition effect.

Conclusions

Due to its significant economic and safety implications, research into corrosion prevention and mitigation is essential. Chitosan-based coatings, including those crosslinked with PEG, and PVP were prepared and characterized. The contact angles obtained in the study indicate that the coatings displayed hydrophilic behavior. The ATR-FTIR spectra analysis showed a significant correlation between chitosan and the crosslinking agents, suggesting a strong bond between these components in the coatings. The AFM results for roughness (Ra) of the samples before and after the coating process indicate a strong relation between the decrease in the roughness parameter and the enhancement of the barrier protective property. Weight loss percentages

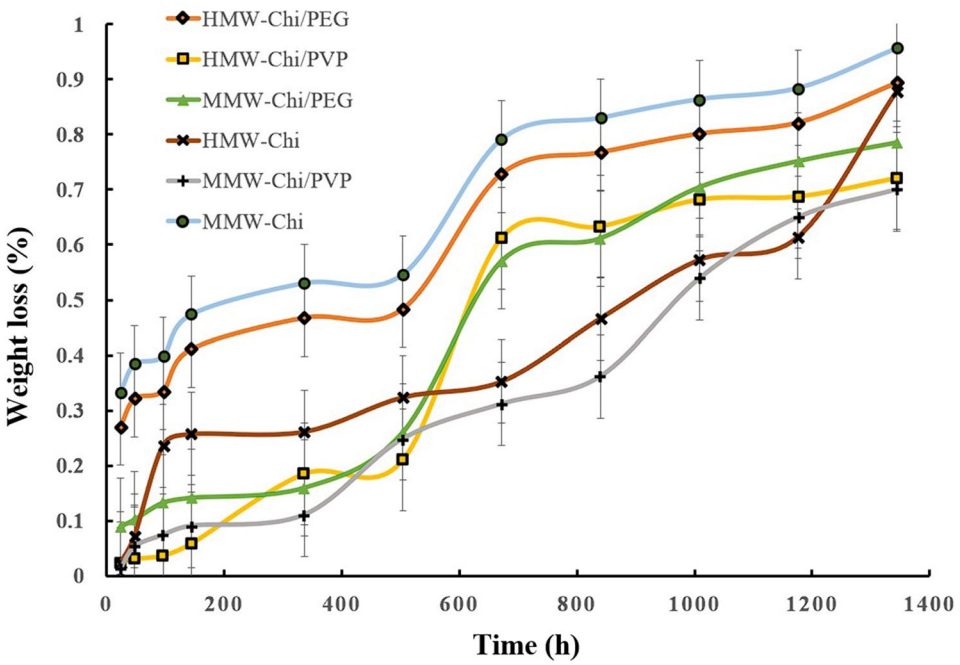

Fig. 2 Weight loss measurements (%) for high and medium molecular weight chitosan-based coatings after 1400 h of immersion in a 3.5% NaCl solution

remained consistently low (0.1–0.9%) throughout the experiment, indicating that the coatings maintained their integrity and adherence to the metal surface, providing long-lasting wear protection in an aggressive medium. In summary, the study suggests that chitosan-based green coatings exhibit promising properties for corrosion protection.

Acknowledgments We acknowledge project ITSON PROFAPI-2023-031 and the project CONAHCyT Ciencia de Frontera CF-2023-G-1395, and the first author is grateful to CONACyT (785138).

Author contributions All authors participated in the study's inception and design. AAA-R, RGS-D, and VMO-C were responsible for material preparation, data collection, and analysis. The characterization studies of the samples were carried out by YV-P, GED-I, and JÁ-S, AAA-R initially drafted the manuscript, which was later revised by RGS-D with input from all authors based on earlier versions of the manuscript. The final published version of the manuscript has been reviewed and approved by all authors.

Data availability The datasets generated during and/or analyzed during the current study are available from the corresponding author on reasonable request.

Declarations

Conflict of interest The authors declare no conflict of interest.

References

1. J. C. Espartero, Polymeric materials for corrosion protection in geothermal systems (OhioLINK Electronic Theses and Dissertations Center, 2015), http://rave.ohiolink.edu/etdc/view?acc_num=case1427901218). Accessed 19 Jan 2023
2. S.A. Umoren, U.M. Eduok, Application of carbohydrate polymers as corrosion inhibitors for metal substrates in different media: a review. Carbohydr. Polym. **140**, 314–341 (2016). https://doi.org/10.1016/j.carbpol.2015.12.038
3. F. Gapsari, S. Hidayatullah, P. Hadi Setyarini, K.A. Madurani, H. Hermawan, Egypt. J. Pet. **31**, 25–31 (2022). https://doi.org/10.1016/j.ejpe.2022.02.001
4. A.M. Motlatle, T.G. Mofokeng, M.R. Scriba, V. Ojijo, S.S. Ray, Synth. Met. (2021). https://doi.org/10.1016/j.synthmet.2021.116914
5. P. Sambyal, G. Ruhi, S.K. Dhawan, B.M.S. Bisht, S.P. Gairola, Prog. Org. Coat. **119**, 203–213 (2018). https://doi.org/10.1016/j.porgcoat.2018.02.014
6. J. Carneiro, J. Tedim, M. G. S. Ferreira, in *Progress in Organic Coatings* (Elsevier B.V., 2015), vol. 89, pp. 348–356 https://doi.org/10.1016/j.porgcoat.2015.03.008
7. Y. Cao, H. Wu, X. Wang, G. Wang, H. Yang, J. Mol. Liq. (2022). https://doi.org/10.1016/j.molliq.2022.119341
8. S. Peter, N. Lyczko, D. Gopakumar, H.J. Maria, A. Nzihou, S. Thomas, Waste Biomass Valor. **12**, 4777–4804 (2021). https://doi.org/10.1007/s12649-020-01244-6
9. M. Martinez-Gomez, A. Quinto-Hernandez, N.S. Flores-Garcia, J. Mayén, M. Dominguez-Diaz, H. Martinez, J. Porcayo-Calderon, J.G. Gonzalez-Rodriguez, L. Martinez-Gomez, Int. J. Polym. Sci. (2019). https://doi.org/10.1155/2019/3864835
10. C. Ardean, C.M. Davidescu, N.S. Nemeş, A. Negrea, M. Ciopec, N. Duteanu, P. Negrea, D. Duda-Seiman, V. Musta, Int. J. Mol. Sci. **22**, 7449 (2021). https://doi.org/10.3390/ijms22147449
11. J.A. Oliveira, R.A. de Santana, A.D. Neto, Prog. Org. Coat. (2020). https://doi.org/10.1016/j.porgcoat.2020.105631
12. Á.F. Szőke, G.S. Szabó, Z. Hórvölgyi, E. Albert, L. Gaina, L.M. Muresan, Carbohydr. Polym. **215**, 63–72 (2019). https://doi.org/10.1016/j.carbpol.2019.03.077
13. R.G. Sánchez-Duarte, D.I. Sánchez-Machado, J. López-Cervantes, M.A. Correa-Murrieta, Water Sci. Technol. **65**, 618–623 (2012). https://doi.org/10.2166/wst.2012.900
14. Á.F. Szőke, G. Szabó, Z. Simó, Z. Hórvölgyi, E. Albert, A.G. Végh, L. Zimányi, L.M. Muresan, Eur. Polym. J. **118**, 205–212 (2019). https://doi.org/10.1016/j.eurpolymj.2019.05.057
15. A.A. Aguilar-Ruiz, G.E. Dévora-Isiordia, R.G. Sánchez-Duarte, Y. Villegas-Peralta, V.M. Orozco-Carmona, J. Álvarez-Sánchez, Coatings **13**, 1615 (2023). https://doi.org/10.3390/coatings13091615
16. S.A. Umoren, A.A. AlAhmary, Z.M. Gasem, M.M. Solomon, Int. J. Biol. Macromol. **117**, 1017–1028 (2018). https://doi.org/10.1016/j.ijbiomac.2018.06.014
17. J. F. Solano Romero, Obtención de quitosano a partir del exoesqueleto del camarón (infraorden caridea), (Repositorio Digital UTMACH, 2017), http://repositorio.utmachala.edu.ec/handle/48000/11382. Accessed 21 Jan 2023
18. I.D. Gunbas, U. Aydemir Sezer, S. Gülce İz, I. Deliloğlu Gürhan, N. Hasirci, Ind. Eng. Chem. Res. **51**, 11946–11954 (2012). https://doi.org/10.1021/ie3015523
19. J. J. Ojeda, M. Dittrich, Methods Mol. Biol. **881**, 187–211 (2012)
20. Q.H. Zhang, B.S. Hou, Y.Y. Li, G.Y. Zhu, H.F. Liu, G.A. Zhang, Corros. Sci. (2020). https://doi.org/10.1016/j.corsci.2019.108346
21. R. Padash, G.S. Sajadi, A.H. Jafari, E. Jamalizadeh, A.S. Rad, Mater. Chem. Phys. (2020). https://doi.org/10.1016/j.matchemphys.2020.122681
22. S.M. Alves, W. Albano, A.J. de Oliveira, J. Braz. Soc. Mech. Sci. Eng. **39**, 845–856 (2017). https://doi.org/10.1007/s40430-016-0545-3
23. S.S. Latthe, P. Sudhagar, A. Devadoss, A.M. Kumar, S. Liu, C. Terashima, K. Nakata, A. Fujishima, J. Mater. Chem. A Mater. **3**, 14263–14271 (2015). https://doi.org/10.1039/c5ta02604k
24. V. Srivastava, D.S. Chauhan, P.G. Joshi, V. Maruthapandian, A.A. Sorour, M.A. Quraishi, ChemistrySelect **3**, 1990–1998 (2018). https://doi.org/10.1002/slct.201701949
25. H. Ashassi-Sorkhabi, A. Kazempour, Chitosan, its derivatives and composites with superior potentials for the corrosion protection of steel alloys: a comprehensive review. Carbohydr. Polym. (2020). https://doi.org/10.1016/j.carbpol.2020.116110